 doi:10.20944/preprints202206.0358.v1

Article

Unsteady Natural Convection in An Initially Stratified Air-filled Trapezoidal Enclosure Heated from below

Md. Mahafujur Rahaman[1,2], Sidhartha Bhowmick[1], Rabindra Nath Mondal[1] and Suvash C. Saha[3,*]

[1] Department of Mathematics, Jagannath University, Dhaka 1100, Bangladesh
[2] Department of Computer Science and Engineering, Z. H. Sikder University of Science and Technology, Shariatpur 8024, Bangladesh
[3] School of Mechanical and Mechatronic Engineering, University of Technology Sydney, Ultimo, NSW 2007, Australia
*Corresponding author: suvash.saha@uts.edu.au

Abstract: Natural convection is intensively explored, especially in a valley-shaped trapezoidal enclosure, because of its broad presence in both technical settings and nature. This study deals with a trapezoidal cavity, which is initially filled with linearly stratified air. Though the side walls remain adiabatic, the bottom wall is heated, and the top wall is cooled. For the stratified fluid (air), the temperature of the fluid adjacent to the top and the bottom walls is the same as that of the walls. Natural convection in the trapezoidal cavity is simulated in two dimensions using numerical simulations, by varying Rayleigh numbers (Ra) from 10^0 to 10^8 with constant Prandtl number, Pr = 0.71, and aspect ratio, A = 0.5. According to numerical results, the development of transient flow within the enclosure owing to the predefined conditions for boundary may be categorized into three distinct stages: early, transitional, and steady or unsteady. The flow characteristics at each of the three phases and the impact of the Rayleigh number on the flow's growth are stated in this study. In addition, heat transfer through the bottom and the top surfaces is described in this study.

Keywords: stratified air; trapezoidal cavity; natural convection; heat transfer; transient flow

1. Introduction

In an enclosure, natural convection has gained a lot of interest among academics since it can be found in a variety of applications and has a big impact on thermal characteristics. Natural convection has been studied inside various shapes of enclosures with numerous boundary conditions to investigate thermal behavior as well as fluid flow, as natural convection is used in an array of technical applications, ranging from geophysics, geothermal reservoirs, building insulation to industrial separation processes and so forth. Unsteady natural convection in a differentially heated cavity has attracted a lot of attention in the scientific literature. Many researchers [1-6] provided comprehensive investigations for regular enclosures (e.g. rectangular, square and triangular) using various numerical models, indicating that multiple investigations have been made to gain a fundamental understanding of unsteady natural convection flows and heat transfer characteristics in an enclosure.

Due to the importance of attics for occupant thermal comfort in buildings, and the resulting energy costs for heating and air conditioning, increased research activities have been carried out on subjects related to heat transfer in attics over the last forty years. Saha et al. [7,8] has examined heat transport through attics under periodic thermal forcing and cooling inclined walls. Natural convection flows within V-shaped triangle enclosures with opposite boundary conditions appeared to be well-studied due to their natural presence. Transitions from symmetric steady to asymmetric unsteady flow were studied by Bhowmick et al. [9,10] in a V-shaped triangular enclosure heated from below and cooled from the top for both air and water. Different flow mechanisms have found for the

Preprints (www.preprints.org) | NOT PEER-REVIEWED | Posted: 27 June 2022 doi:10.20944/preprints202206.0358.v1

different fluids. Wang et al. [11] has experimented with natural convection in a V-shaped enclosure with the same boundary conditions of [10].

Any triangular, square, or rectangular cavity is inadequate for numerous engineering systems as well as geophysical circumstances where the enclosure geometry varies or contains extra tending walls. Natural convection in a trapezoidal enclosure is far more difficult to examine than in any regular enclosures because of the sloped walls. This complicated geometry needs a precise and large effect in mesh creation and code development. However, there were a number of studies on natural convection that focused on trapezoidal enclosures. Iyican et al. [12,13] has considered trapezoidal cavity with boundary conditions of heated base wall and parallel cylindrical cooled top wall to investigate natural convection of the cavity, using experimental and computational methods. Lee [14] has reported a theoretical and experimental investigation of the non-rectangular enclosure, in which two 45° inclined sides of a trapezoidal cross-section were chosen, with different heating conditions. Lam et al. [15] has found analogous findings for a trapezoidal enclosure with cooled inclined top wall, heated bottom wall, and insulated vertical sidewalls.

Lee [16] has numerically examined the fluid flow and the heat transfer which were passed through a cold chamber of a trapezoidal enclosure, where heated fluid was supposed to flow into one end of the chamber from a depth below the surface and was removed from the other end at a different depth. Lee [17] and Peri [18] have showed numerical findings in the case of laminar natural convection within a trapezoidal cavity with inclined sidewalls kept at varying constant temperatures, and adiabatic top and base walls for the $Ra \leq 10^6$. Sadat and Salagnac [19] have used a finite element based on the control-volume approach to compute the similar geometry for Rayleigh numbers from 10^3 to 2×10^5. Kuyper and Hoogendoorn [20] have examined laminar natural convection flow within a trapezoidal cavity in order to see the effect of the flow by the inclination angle, and the relationship between the Ra and the average Nu. Moukalled and Darwish [21] have looked at how heat transfer was affected by installing baffles upon the top inclined walls inside trapezoidal cavities. Boussaid et al. [22] has examined thermal heat transfer inside a trapezoidal chamber in which the base wall was heated and the tending upper half was cooled. The influence of natural convection flow within a trapezoidal cavity was examined by Natarajan et al. [23] under the conditions of a heated base wall as well as linearly heated and cooled vertical walls, but with no insulation on the top wall. Hammami et al. [24] has investigated the fixed heat and mass transport processes within a trapezoidal enclosure using a binary air-water vapor mixture. Later, Natarajan et al. [25] has explored natural convection flow inside a trapezoidal cavity in which, on the one hand, the base wall was, both consistently and inconsistently, warmed and the upward walls were, through a steady temperature shower, kept cool, and then again, the upper wall remains insulated. Basak et al. [26] has examined natural convection energy fluxes in trapezoidal enclosures in which the top walls were insulated, whereas the bottom walls were heated, and sidewalls were cooled.

For three vertex angles in trapezoidal isosceles, the advancement of natural convection oscillatory flow patterns was examined by Noah and Daniel [27]. Mustafa and Ghani [28] have explored a natural convection flow inside a trapezoidal cavity with partially heated bottom wall and cooled vertical walls through a constant temperature bath, and a well-insulated top wall. By means of the 'Element based Finite Volume Method', Silva et al. [29] has studied natural convection inside trapezoidal enclosures. Gholizadeh et al. [30] has explored the natural convection inside a trapezoidal enclosure where the right inclined wall was partially heated, by means of the finite difference method. In a porous trapezoidal enclosure saturated through a power-law non-Newtonian fluid, Yazdani et al. [31] has considered natural convection as well as entropy production. To better comprehend the effect of heating length on the active bottom wall, Gowda et al. [32] has observed natural convection within the cavity of a trapezoid under the condition that the base wall was partly heated, upper wall was adiabatic and the inclined wall remains at a fixed cooled temperature.

Preprints (www.preprints.org) | NOT PEER-REVIEWED | Posted: 27 June 2022 doi:10.20944/preprints202206.0358.v1

Various boundary conditions were used in the trapezoidal cavity by various researchers, according to the above literature studies. However, an initially stratified air-filled trapezoidal enclosure, is still ambiguous, which encourages the conducting of this research. It has direct application to environmental fluid dynamics which deals with the heat transfer and airflow process in the thermal stratification environment. This using two-dimensional numerical simulations for Ra = 10^0 to 10^8, Pr = 0.71, and A = 0.5, the transitional flow in the trapezoidal cavity is considered in this article. The influence of Ra on fluid flow and heat transfer is thoroughly examined.

Nomenclature

A	aspect ratio	ΔT	temperature difference, $(T_h - T_c)$
g	gravitational force (m/s^2)	k	thermal conductivity (W/(m·K))
L, H	half-length and height of the enclosure (m)	u, v	dimensional velocity components (m/s)
ln	dimensionless length of the horizontal wall	U, V	dimensionless velocity components
n	dimensionless coordinate normal to the horizontal wall	x, y	dimensional horizontal and vertical coordinates
t	time (s)	X, Y	dimensionless horizontal and vertical coordinates
Nu	Nusselt number		
P	Pressure (N/m^2)	β	thermal expansion coefficient (1/K)
Pr	Prandtl number		
Ra	Rayleigh number, $g\beta(T_h-T_c)H^3/\nu\kappa$	κ	thermal diffusivity (m^2/s)
T	dimensional temperature (K)	ν	kinematic viscosity (m^2/s)
T_∞	dimensional ambient temperature (K)	ρ	density (kg/m^3)
T_h	dimensional temperature of the heated bottom wall (K)	τ	dimensionless time
		$\Delta\tau$	dimensionless time step
T_c	dimensional temperature of the cooled top wall (K)	θ	dimensionless temperature

2. Problem formulations

This study considers a trapezoidal enclosure of height H, as well as the horizontal length of the top, $2L$, where $L = 2H$; i.e., $A = H/L = 0.5$. Fig. 1 illustrates a non-dimensional physical model with boundary conditions. A tiny percentage (= 4% of L) of each top corner is sliced to dispense with the singularity around the position between inclination and upper walls, and cutting walls are subject to an adiabatic thermal state. The fluid in the cavity with Pr = 0.71 is considered, which is, in the beginning, linearly stratified as having the highest $T = T_h$ temperature at the bottom and the lowest $T = T_c$ temperature at the top. The boundaries are non-slip.

Preprints (www.preprints.org) | NOT PEER-REVIEWED | Posted: 27 June 2022 doi:10.20944/preprints202206.0358.v1

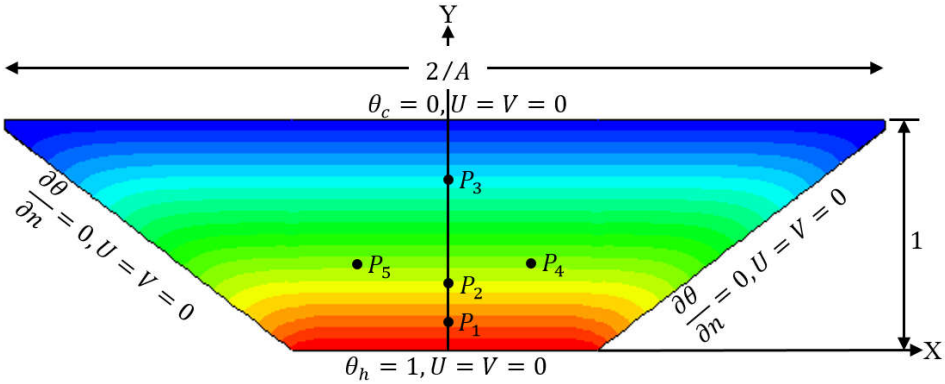

Figure 1. Schematic of physical domain with non-diensional boundary conditions with the monitoring points P_1 (0, 0.133), P_2 (0, 0.4), P_3 (0, 0.8), P_4 (0.4, 0.51) and P_5 (-0.4, 0.51), which are utilized in the resulting figures.

In a trapezoidal enclosure, natural convection of stratified air is assumed. The subsequent set of governing equations with the Boussinesq approximation regulate the progress of natural convection flows in the enclosure:

$$\frac{\partial u}{\partial x} + \frac{\partial v}{\partial y} = 0, \tag{1}$$

$$\frac{\partial u}{\partial t} + u\frac{\partial u}{\partial x} + v\frac{\partial u}{\partial y} = -\frac{1}{\rho}\frac{\partial p}{\partial x} + \nu\left(\frac{\partial^2 u}{\partial x^2} + \frac{\partial^2 u}{\partial y^2}\right), \tag{2}$$

$$\frac{\partial v}{\partial t} + u\frac{\partial v}{\partial x} + v\frac{\partial v}{\partial y} = -\frac{1}{\rho}\frac{\partial p}{\partial y} + \nu\left(\frac{\partial^2 v}{\partial x^2} + \frac{\partial^2 v}{\partial y^2}\right) + g\beta(T - T_0), \tag{3}$$

$$\frac{\partial T}{\partial t} + u\frac{\partial T}{\partial x} + v\frac{\partial T}{\partial y} = \kappa\left(\frac{\partial^2 T}{\partial x^2} + \frac{\partial^2 T}{\partial y^2}\right). \tag{4}$$

The followings are the dimensionless variables that were used:

$$X = \frac{x}{H}, \quad Y = \frac{y}{H}, \; U = \frac{uH}{\kappa}, \; V = \frac{vH}{\kappa}, \; P = \frac{pH^2}{\rho\kappa^2}, \; \theta = \frac{T - T_\infty}{T_h - T_c}, \; \tau = \frac{t\kappa}{H^2}. \tag{5}$$

The three governing parameters, which are aspect ratio (A), Pr and Ra [33], influence the natural convective flows in the enclosure that can be expressed as follows:

$$Ra = \frac{g\beta(T_h - T_c)H^3}{\nu\kappa}, Pr = \frac{\nu}{\kappa}, A = \frac{H}{\mathrm{L}}. \tag{6}$$

After adding the aforementioned dimensionless variables equations (1) to (4) become,

$$\frac{\partial U}{\partial X} + \frac{\partial V}{\partial Y} = 0, \tag{7}$$

$$\frac{\partial U}{\partial \tau} + U\frac{\partial U}{\partial X} + V\frac{\partial U}{\partial Y} = -\frac{\partial P}{\partial X} + Pr\left(\frac{\partial^2 U}{\partial X^2} + \frac{\partial^2 U}{\partial Y^2}\right), \tag{8}$$

$$\frac{\partial V}{\partial \tau} + U\frac{\partial V}{\partial X} + V\frac{\partial V}{\partial Y} = -\frac{\partial P}{\partial Y} + Pr\left(\frac{\partial^2 V}{\partial X^2} + \frac{\partial^2 V}{\partial Y^2}\right) + PrRa\theta, \tag{9}$$

$$\frac{\partial \theta}{\partial \tau} + U\frac{\partial \theta}{\partial X} + V\frac{\partial \theta}{\partial Y} = \frac{\partial^2 \theta}{\partial X^2} + \frac{\partial^2 \theta}{\partial Y^2}. \tag{10}$$

Preprints (www.preprints.org) | NOT PEER-REVIEWED | Posted: 27 June 2022 doi:10.20944/preprints202206.0358.v1

3. Time step and grid dependent tests

In this study, ANSYS FLUENT 17.0, a finite-volume-based fluid simulation software, is used to enable the high Rayleigh number flows (Armfield and Street [34-36]). In order to find solutions to the governing Equations (7-10), and other conditions, the SIMPLE scheme is used. Using the QUICK scheme (see Leonard and Mokhtari [37]), we discretized the advection term. We have also used central differencing along with second-order accuracy to discretize the diffusion terms. Moreover, a second-order implicit time-marching scheme is employed for the unsteady term.

Table 1. Temperature at P_2 (0, 0.4) employing various grids and time steps.

Grids and time steps	Average value of the temperature	Percentage of the variance
225×75 and $\Delta\tau = 0.01$	0.306495	1.42%
300×100 and $\Delta\tau = 0.01$	0.310895	-
300×100 and $\Delta\tau = 0.005$	0.313003	0.68%
375×125 and $\Delta\tau = 0.01$	0.309845	0.34%

We have also performed the grid and time step dependency test for the greatest Rayleigh number, Ra = 10^8 used in this study. We have created three symmetrical meshes of 225×75, 300×100 and 375×125, which are non-uniform using the application ANSYS ICEM, by way of coarser grids in the interior area as well as finer grids around the edges. From a width of at least 0.002 adjacent to the wall to the width of 0.02 in the interior, the mesh of 300×100 has been increased at a rate of 3%. At position P_2 (0, 0.4), employing various grids together with time steps, the temperature time series is computed for Ra = 10^8 as depicted in Fig.2. The results evidently show that temperatures predicted with various meshes and time steps are constant in the initial phases, but somewhat deviate in the fully matured stage. Table 1 shows the temperature averaged at the fully-developed phase once more.

The differences in the results produced using different meshes and time steps can be shown to be less than 2%, which is satisfactory. Considering the computational cost, a mesh of 300×100 and a time step of 0.01 were used in numerical simulation.

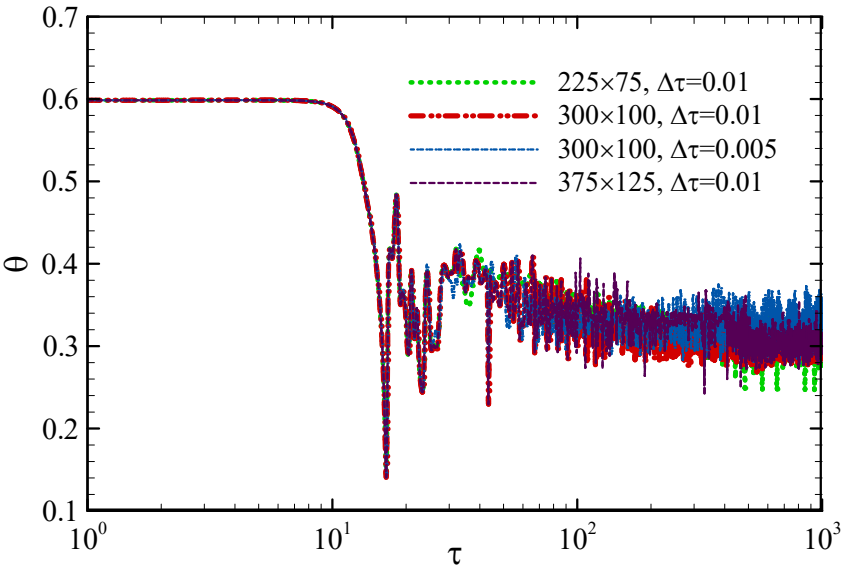

Figure 2. Temperature time series at P_2 (0, 0.4) for Ra = 10^8 with distinct grids as well as time steps.

Preprints (www.preprints.org) | NOT PEER-REVIEWED | Posted: 27 June 2022 doi:10.20944/preprints202206.0358.v1

4. Results and discussions

For Ra = 10^0 to 10^8, Pr = 0.71 and A = 0.5, we have explained the transient evolution of the flow in an initially stratified air-filled trapezoidal cavity in response to consistent heating through the base and similar cooling via the top surfaces using computational fluid dynamics approach.

4.1. Development of the transient flow

For Ra = 10^0 to 10^2, we have found that there is no ascending or descending plume in the flow development, i.e., the flow is always steady under a conduction dominance for those Rayleigh numbers. For the sake of brevity, results are not presented here for Ra = 10^0 to 10^2. So that, for Ra = 10^3 to 10^8, the general characteristics of flow development in a trapezoidal enclosure are presented (see Figs. 3-5) here. The development of the flow for these Rayleigh numbers, according to the numerical simulations, may be divided into the following: early-stage, transitional stage, and steady or unsteady stage.

4.1.1. Flow at the early stage

In the trapezoidal enclosure, the air is at first stratified, as indicated in the preceding sections. At the beginning of the numerical studies, the instant conditions for isotherms are created across the surfaces that first cool the cavity via the upper surface and then make it warm through the bottom. Thermal boundary layer forms along all internal surfaces as a result. The cooling thermal boundary layer is near the top wall, whereas the heating thermal boundary layer is alongside the bottom surface. The lower section produces the heating thermal boundary layer, while the top section of the upper layer produces the cooling thermal boundary layer. The progress of the thermal boundary layers through time is depicted in Fig. 3, exhibiting isotherms and streamlines (Fig. 3a-3e) at τ = 6 after start-up.

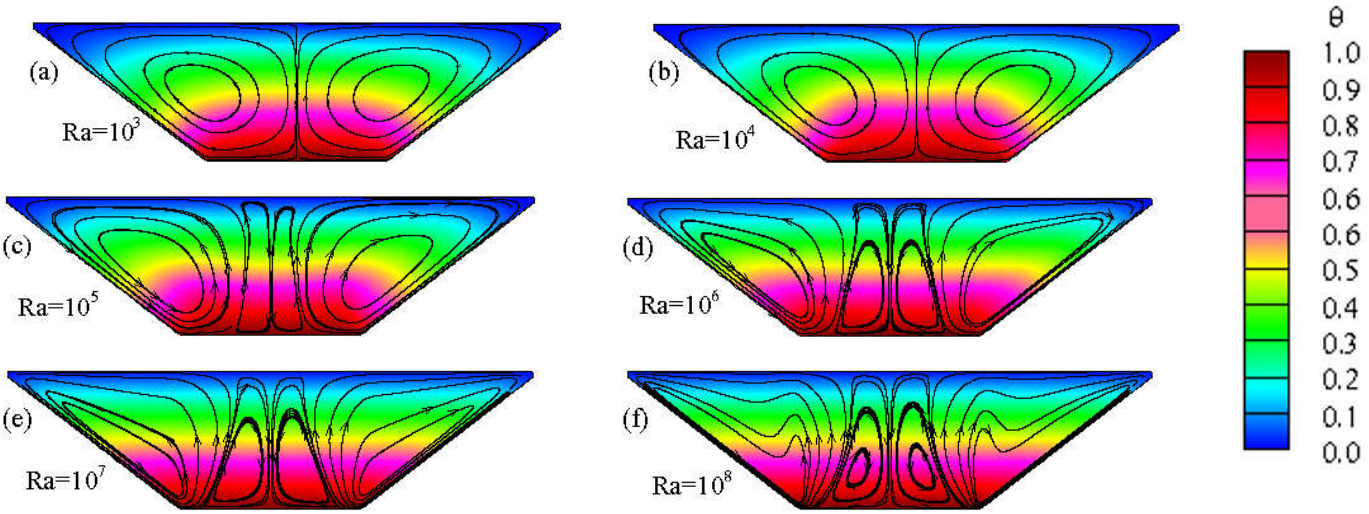

Figure 3. Streamlines and isotherms at the early stage for the different Rayleigh numbers at τ = 6.

At the early stage, the core's fluid stays isothermal, as shown in Fig. 3, in spite of the expansion of the thermal boundary layer, at the initial temperature. Because the bottom part of the enclosure is heated and the top section is cooled, the heated fluid from the bottom travels via the boundary layer towards the upper parts. On the contrary, the boundary layer transports cooled air to the bottom from the top. Both warm and cold fluids meet in the middle of the top wall and release into the core. There remains another heated boundary layer near the bottom section that begins to expand, as the thermal forcing begins. At this moment, the isothermal difference reveals the thicknesses of the thermal layer barrier to the center growing with time. The streamlines show that Ra = 10^3 to 10^5 has two weak revolving cells, and, Ra = 10^6 to 10^8 has four weak rotating cells. The

Preprints (www.preprints.org) | NOT PEER-REVIEWED | Posted: 27 June 2022 doi:10.20944/preprints202206.0358.v1

isotherms and streamlines for different Ra remain symmetric with regard to the cavity's y-axis line at this stage.

4.1.2. Transitional stage

The formation of convective instabilities marks the flow in the form of ascending and descending plumes at the transitional phase. Through the warming of the bottom portion, the horizontal thermal boundary layer, which has warmed air under colder air, is unstable to 'Rayleigh-Bénard instabilities', is formed. When the critical conditions are fulfilled, the hot thermal boundary layer becomes unsteady.

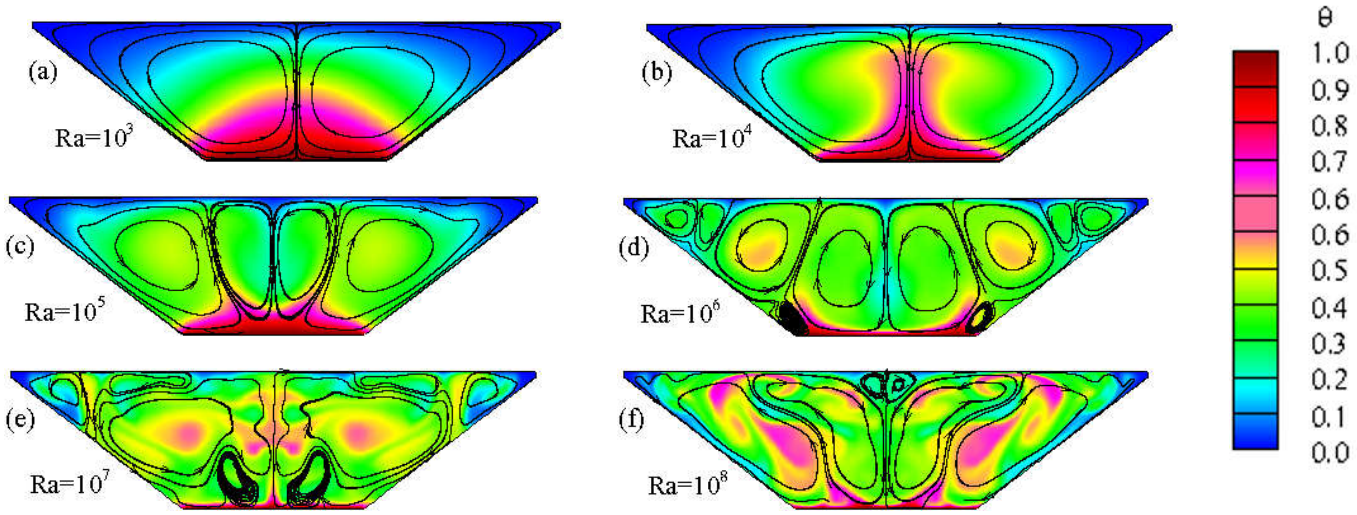

Figure 4. Streamlines and isotherms at the initial transitional stage for the different Rayleigh numbers at $\tau = 20$.

In this regime, Fig. 4 and Fig. 5 display the streamlines and isotherms at various periods. It has previously been noted that when air of two different temperatures passes through the boundary layer around the midpoint of inclined surfaces, it invariably travels downwards. Subsequently, the heated air plume then moves to the cavity's core, while the cooled air plume goes to the lower portion from the upper layer. Fig. 4(a-b) shows that the flow becomes symmetric and steady at $\tau = 20$ for Ra = 10^3 to 10^4. The flow grows stronger and finally asymmetric as time passes due to pitchfork bifurcation. The figures demonstrate the asymmetric isotherms and streamlines for the higher Rayleigh numbers. It is without a doubt significant that with the greater Rayleigh number, the flow oscillates for quite a long period. The bifurcation continues to rehash left and close to the symmetric focal line while oscillating. Fig. 5(c-d) depicts that the flow becomes symmetric and steady at $\tau = 100$ for Ra = 10^5 to 10^6. Because of the presence of convective instabilities, the rotating cells that are at the beginning of the growth of the flow are fragmented into several cells, which is demonstrated in Fig. 4 and Fig. 5 by the outlines of the isotherms and streamlines.

Preprints (www.preprints.org) | NOT PEER-REVIEWED | Posted: 27 June 2022 doi:10.20944/preprints202206.0358.v1

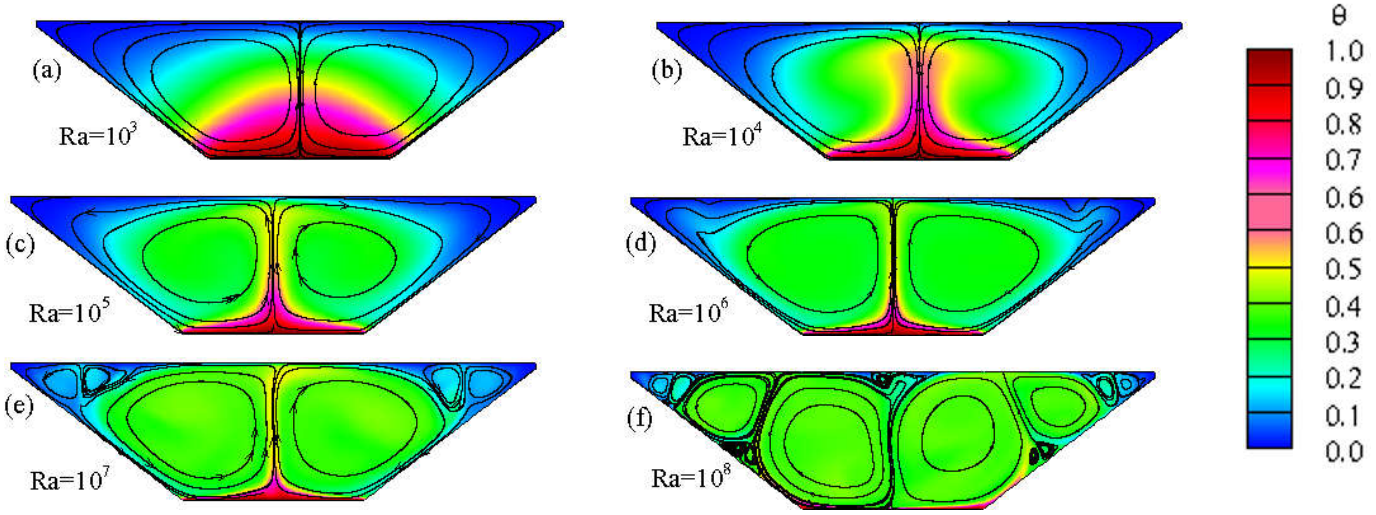

Figure 5. Streamlines and isotherms at the developed transitional stage for the different Rayleigh numbers at $\tau = 100$.

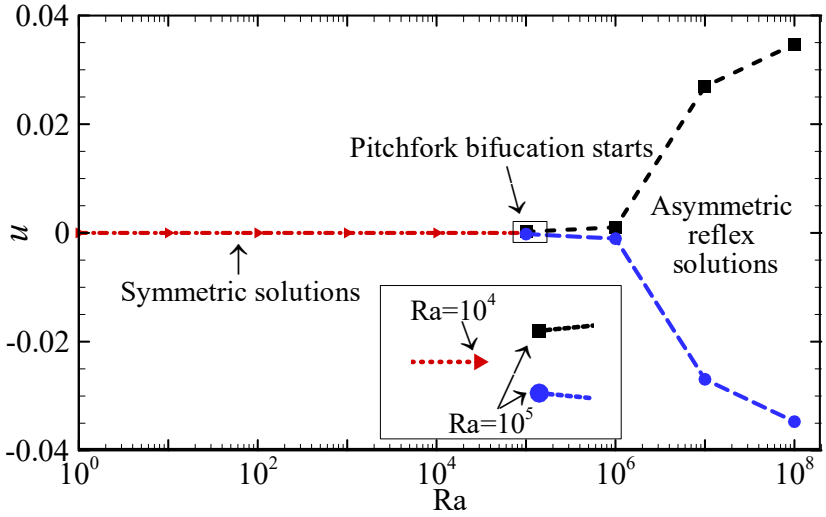

Figure 6. Pitchfork bifurcation in the Ra-u plane where u is the x-velocity at the point, P_3 (0, 0.8).

A pitchfork bifurcation starts to happen due to the results of Rayleigh-Bénard instability. The x-velocity at point P_3 (0, 0.8) in the Ra-u plane is provided in Fig. 6 to explain such a Pitchfork bifurcation from symmetric to asymmetric state at the completely developed stage ($\tau = 1000$). Because the flow is symmetric around the y-axis and point P_3 is on the y-axis, the x-velocity for $Ra < 10^5$ is close to zero. When the Rayleigh number surpasses or equivalents to 10^5, the cell inclines to the right side with the increment of the x-velocity, as set apart by the square line however to the left side with the reduction of the x-velocity, as set apart by the circle line in Fig. 6.

4.1.3. Flow at the steady or unsteady stage

In the late transitional phase, a pitchfork bifurcation occurs, resulting in the formation of an asymmetric flow structure. The pitchfork bifurcation occurs early in the numerical simulation, as previously mentioned.

Preprints (www.preprints.org) | NOT PEER-REVIEWED | Posted: 27 June 2022 doi:10.20944/preprints202206.0358.v1

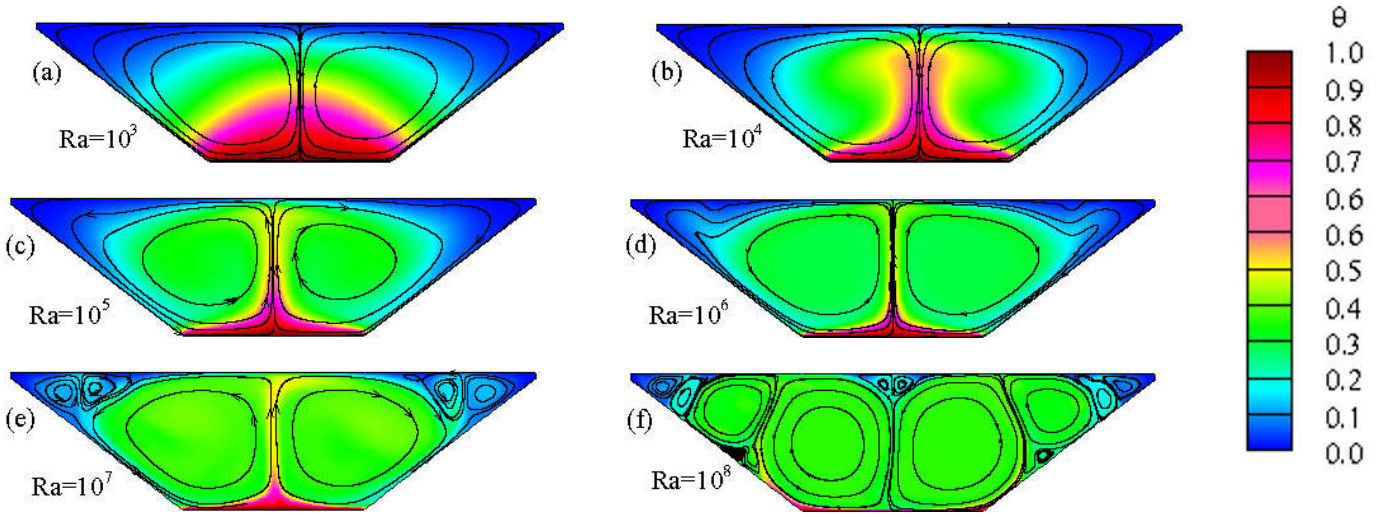

Figure 7. Streamlines and isotherms at the fully developed stage for the different Rayleigh numbers at $\tau = 2000$.

The convective instabilities alternate on either side of the cavity, and the upward-moving heated air plumes on the base side appear in the middle at different times, which is a fascinating event as shown in the numerical simulation. During the transitional stage, the flow, on the other hand, has multiple undershoots and overshoots prior to becoming completely stable. Thermal travels from the boundary layer on either side of the portion discharge fluid to the cavity's centre over time. At the fully developed phase, the fluid inside the enclosure reaches a steady-state for Ra = 10^3 to 10^6 (see Fig. 7a-7d). If Ra ≤ 10^6 Fig. 7(a-d) reveal that the flow becomes stable under various initial conditions. Furthermore, for Ra ≥ 10^7, Fig. 7(e-f) depicts isotherms and streamlines. Fig. 7(e) represents a few tiny cells forming on the top right and left sides of the larger cell. However, when looking at the numerical data, it can be seen that the two tiny cells alternately emerge, indicating that the flow arrives unsteady state at a fully advanced stage for Ra = 10^7. With the increase of Ra, however, both the cells develop in the center of the two biggest cells, as seen in Fig. 7(f). In Fig. 7(f), for Ra = 10^8, the biggest cell in the center also travels between right and left. As a result, the unsteady flow gets more complicated.

To comprehend the unstable flow for greater Rayleigh numbers, the series of temperature-time is presented in Fig. 8. It is apparent that, at the completely advanced stage, the flow is stable as shown in Fig. 8(a), and that the flow pattern in Fig. 8(b) concurs with the finding of a Hopf bifurcation from a steady state to periodic condition. With the increase of Ra, the periodic flow fluctuates, as well as the unstable flow turns chaotic for Ra = 10^8. This is illustrated in Fig. 8(c).

Preprints (www.preprints.org) | NOT PEER-REVIEWED | Posted: 27 June 2022 doi:10.20944/preprints202206.0358.v1

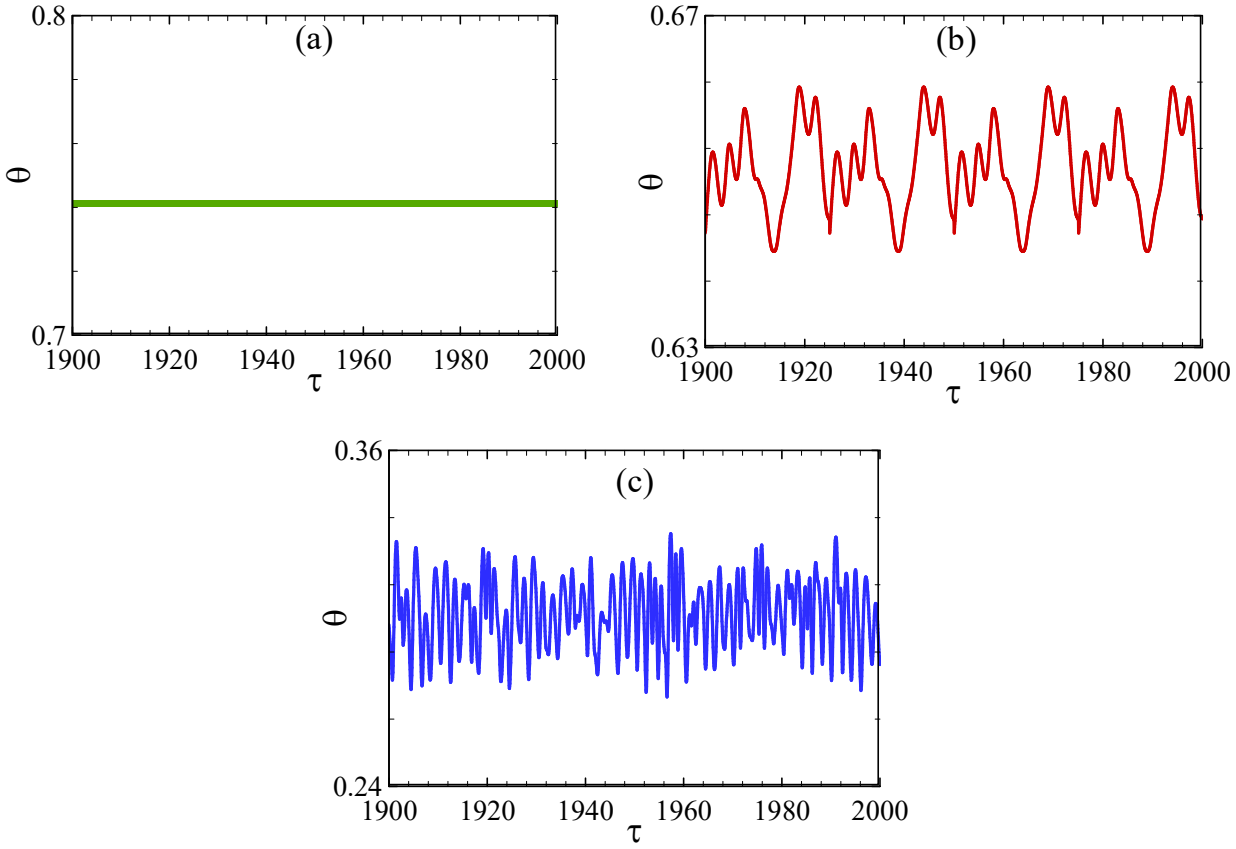

Figure 8. At the fully developed stage, temperature time series at point P_3 (0, 0.8) for (a) Ra = 10^6, (b) Ra = 10^7 and (c) Ra = 10^8.

To comprehend the Hopf bifurcation, which occurs at the transition from steady to periodic phase, the attractors (τ = 300 to 2000) for Ra = 10^6 and (τ = 1000 to 2000) for Ra = 10^7 at the point P_4 (0.4, 0.51), are depicted in Fig. 9. In Fig. 9(a), the curve in the u-θ plane is clearly nearing a certain value with the passage of time for Ra = 10^6. In contrast, Fig. 9(b) shows a limit cycle for Ra = 10^7 (dense curve). Consequently, a Hopf bifurcation occurs at Ra = 10^7 (referred to [38] for a full description of Hopf bifurcation).

At point P_3 (0, 0.8) for Ra = 10^7 and 10^8, the directions of phase-space of the u-θ plane are depicted in Fig. 10 with a view to demonstrating the transformation to chaotic from the periodic condition in greater detail. In Fig. 10(a), the limit cycle can be seen, indicating that the unsteady flow is periodic for Ra = 10^7, which is compatible with Fig. 8. In Fig. 10(b), the trajectory turns out to be chaotic for Ra = 10^8, indicating that the periodic flow transforms into chaotic which happens within Ra = 10^7 and 10^8. This has been referred to [39] for a full description of the phase-space trajectories.

Preprints (www.preprints.org) | NOT PEER-REVIEWED | Posted: 27 June 2022 doi:10.20944/preprints202206.0358.v1

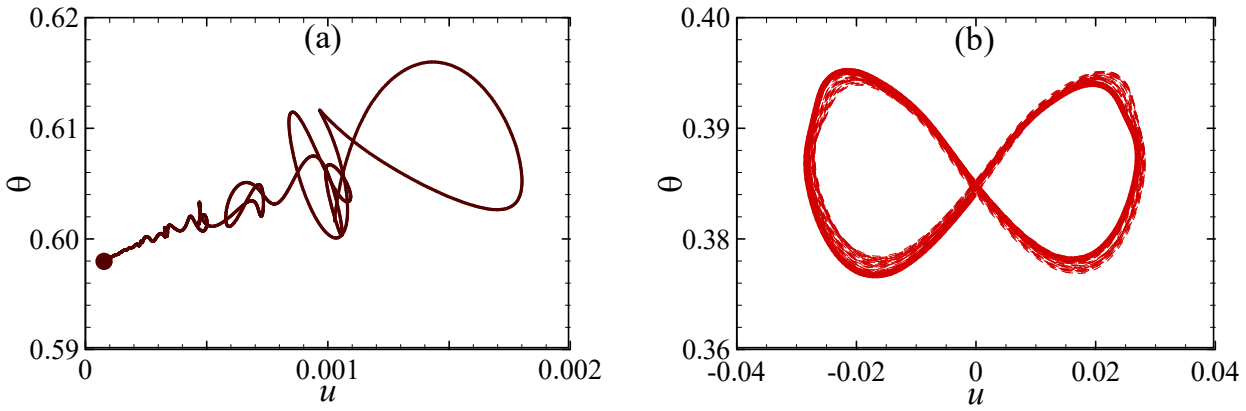

Figure 9. Limit point and limit cycle in the u-θ plane at the point P_4 (0.4, 0.51) respectively for (a) Ra = 10^6 and (b) Ra = 10^7.

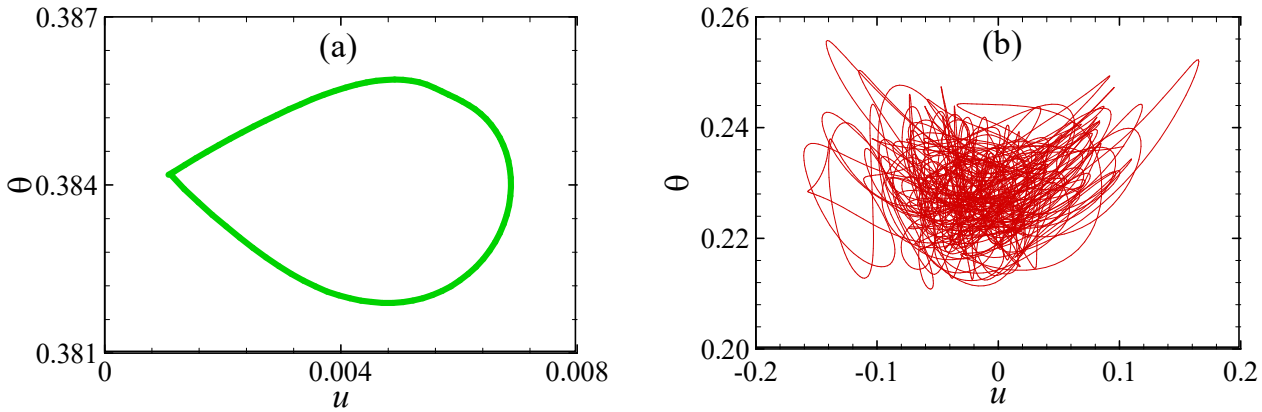

Figure 10. Phase-space trajectories in the u-θ plane at the point P_5 (-0.4, 0.51) for (a) Ra = 10^7 and (b) Ra = 10^8.

4.2. Impact of Rayleigh numbers on the progress of the flow

An array of Rayleigh numbers, ranging from Ra = 10^3 to 10^8, has been used in the simulations. An observation has been made in the different transient flow characteristics throughout an array of Rayleigh numbers. For A = 0.5, the isotherms and accompanying streamlines are depicted in Figs. 3-6 for different Rayleigh numbers. The numerical findings for the various Rayleigh numbers, as shown in Fig. 11, reveal some differences. To begin with, convective flow instabilities can be noticed at the lowermost Rayleigh number. However, with a higher Rayleigh number, the unsteadiness becomes more pronounced, as well as the corresponding wave number rises. For Ra = 10^3 to 10^4, the flow is weaker and symmetric behavior is visible, which is expected; i.e., the flow is symmetric and constant. The flow becomes asymmetric for Ra = 10^5 and 10^6 in the transitional stage and becomes steady at the fully developed stage. Finally, for Ra = 10^7 and Ra = 10^8, the flow becomes periodic and chaotic, respectively.

Preprints (www.preprints.org) | NOT PEER-REVIEWED | Posted: 27 June 2022 doi:10.20944/preprints202206.0358.v1

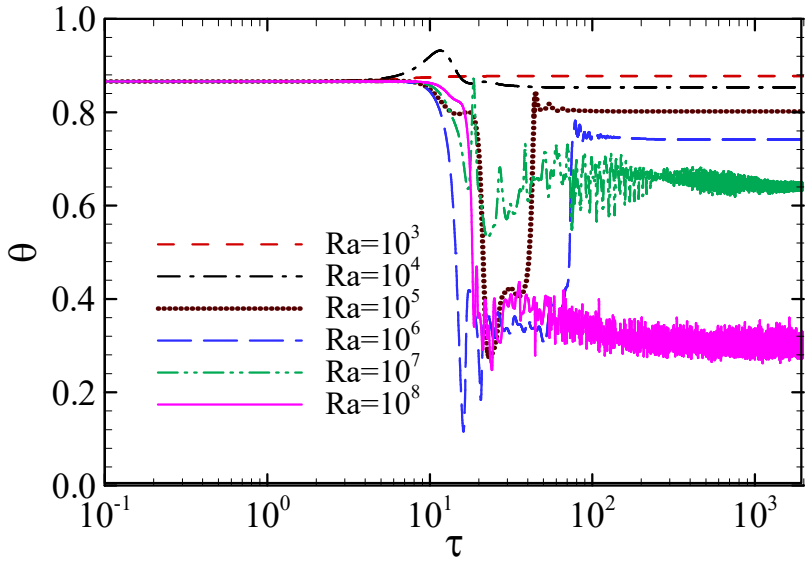

Figure 11. Series of temperature and time at point P_1 (0, 0.133) for various Rayleigh numbers.

5. Heat transfer

The time series of averaged Nusselt number (Nu) of the lower and upper surfaces are calculated and demonstrated in Fig. 12 in order to measure heat transfer through the cavity's wall. At this study, the Nusselt number is defined as (Bhowmick et.al. [40] and Cui et.al. [41]).

$$Nu = \frac{1}{ln}\int_{ln}^{\frac{d\theta}{dn}} ds. \tag{11}$$

The temperature in the internal cavity changes at various periods in the early stages because the fluid in the cavity is initially stratified. As the upper and lower walls are cooled and heated at the same time, but due to the initially stratified fluid no significant distinction in temperature between the fluid observed and the wall might lead to tiny heat transfer and, as a result, a small Nu value is predicted initially. The stratification breaks down with time, and the temperature differential in the interior cavity approaches zero. When the fluid's stratification becomes weaker, then the waviness of Nu is increased with increased of Ra. In the transitional period for larger Ra, the Nu is oscillatory. At the completely developed stage, the Nusselt number is fixed for Ra ≤ 10^6 and oscillatory for Ra ≥ 10^7. These findings are compatible with those in Fig. 11.

Preprints (www.preprints.org) | NOT PEER-REVIEWED | Posted: 27 June 2022 doi:10.20944/preprints202206.0358.v1

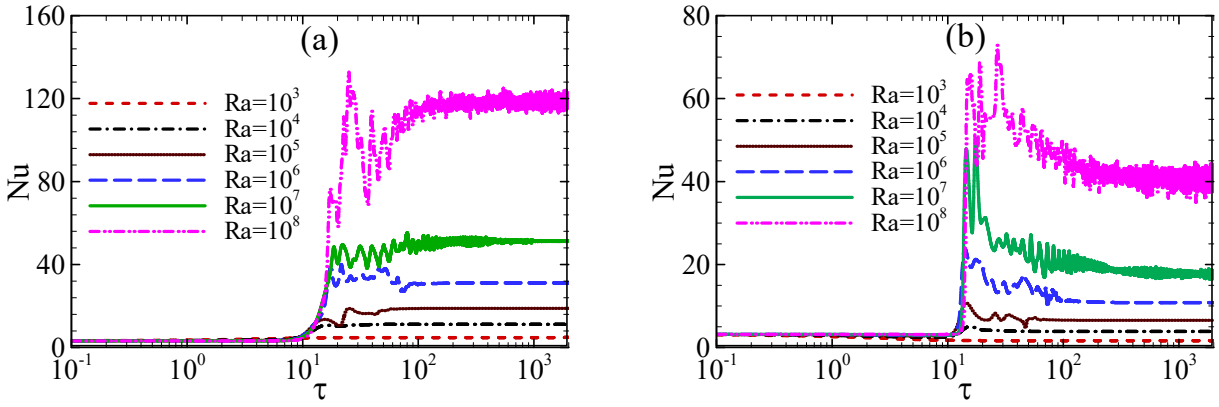

Figure 12. Time series of the Nusselt number for the various Ra on (a) hot bottom wall and (b) cold top wall.

6. Conclusion

This study is concerned with the transient thermal convection in a trapezoidal cavity that is stuffed with linearly stratified air. Though the inclined walls remain adiabatic, the base wall is warmed, and the top wall is cooled with a specified aspect ratio A = 0.5 throughout varieties of Ra (10^0 to 10^8). The finite volume-based FLUENT software has been used to conduct the numerical simulation. The key findings of this study may be described in the following terms:

- According to numerical simulation, the development of transient flow within the enclosure owing to the predefined boundary conditions may be categorized into three separate stages: early, transitional, and steady or unsteady, all of which have been shown in Figs. 3–6.
- The flow at the beginning phase is portrayed through the arrangement of thermal boundary layers close towards every internal surface and the commencement of primary circulations. In the energy conditions, whenever the terms of convection and conduction are adjusted, the flow gets into the transitional state. In the transitional level, the flow is depicted via the base of convective dangers through ascending and descending thermal plumes, as well as the creation of the cellular flow formations. Furthermore, symmetric flows regarding the geometrically symmetric plane for smaller Ra, as well as for relatively higher Ra are characterized by pitchfork bifurcation which represents the flow from symmetry to asymmetry. With respect to the variance in Ra, the time scale for the flow development is likewise computed. For the pitchfork bifurcation, the difference in the behaviour of symmetric flow to asymmetric has additionally been examined.
- For the stratified air, the temperatures of the fluid adjacent to the top and base walls are same as the temperature of the walls. Heat transmission has been studied through the enclosure, as well as the base and top walls, and it has been discovered that, initially, the Nu is small for the stratified air, but after stratification breakup, Nu gradually increases in the transitional stage, and is fixed for Ra ≤ 10^6 and oscillatory for Ra ≥ 10^7 at the completely developed stage.

References

[1] J. Patterson, and J. Imberger, Unsteady natural convection in a rectangular cavity. *Journal of Fluid Mechanics*, *100*(1), 65-86 (1980).

[2] D. Kuhn and P. H. Oosthuizen, Unsteady natural convection in a partially heated rectangular cavity. *Journal of Heat Transfer (Transactions of the ASME (American Society of Mechanical Engineers), Series C);(United States)*, *109*(3),

(1987).

[3] J. Ma and F. Xu, Unsteady natural convection and heat transfer in a differentially heated cavity with a fin for high Rayleigh numbers. *Applied Thermal Engineering*, *99*,625-634, (2016).

[4] X. Wen, L. P. Wang, and Z. Guo, Development of unsteady natural convection in a square cavity under large temperature difference. *Physics of Fluids*, *33*(8), 084108, (2021).

[5] S. C. Saha, Unsteady natural convection in a triangular enclosure under isothermal heating. *Energy and Buildings*, *43*(2-3), 695-703, (2011).

[6] C. Lei, S. W. Armfield and J. C. Patterson, Unsteady natural convection in a water-filled isosceles triangular enclosure heated from below. *International Journal of Heat and Mass Transfer*, *51*(11-12), 2637-2650, (2008).

[7] S. C. Saha, J. C. Patterson and C. Lei, Natural convection and heat transfer in attics subject to periodic thermal forcing. *International Journal of Thermal Sciences*, *49*(10), 1899-1910, (2010).

[8] S. C. Saha, J. C. Patterson and C. Lei, Natural convection in attics subject to instantaneous and ramp cooling boundary conditions. *Energy and Buildings*, *42*(8), 1192-1204, (2010).

[9] S. Bhowmick, S. C. Saha, M. Qiao and F. Xu, Transition to a chaotic flow in a V-shaped triangular cavity heated from below. *International Journal of Heat and Mass Transfer*, *128*, 76-86, (2019).

[10] S. Bhowmick, F. Xu, M. M. Molla and S. C. Saha, Chaotic phenomena of natural convection for water in a V-shaped enclosure. *International Journal of Thermal Sciences*, *176*, 107526 (2022).

[11] X. Wang, S. Bhowmick, Z. F. Tian, S. C. Saha and F. Xu, Experimental study of natural convection in a V-shape-section cavity, *Physics of Fluids*, *33*(1), 014104 (2021).

[12] L. Iyican, Y. Bayazitoglu, and L. C. Witte, An analytical study of natural convective heat transfer within a trapezoidal enclosure. *Journal of Heat Transfer*, 102(3), 640–647 (1980)

[13] L. Iyican, L. C. Witte and Y. Bayazitoglu, An experimental study of natural convection in trapezoidal enclosures. *Journal of Heat Transfer*, 102(3), 648–653 (1980).

[14] T. S. Lee, Computational and experimental studies of convective fluid motion and heat transfer in inclined non-rectangular enclosures. *International journal of heat and fluid flow*, *5*(1), 29-36 (1984).

[15] S. W. Lam, R. Gani and J. G. Symons, Experimental and numerical studies of natural convection in trapezoidal cavities. *Journal of Heat Transfer*, 111(2), 372–377 (1989).

[16] T. S. Lee, Mixed laminar heat and fluid flow in flow-through opened trapezoidal cooling chambers of low aspect ratios. *International Journal of Numerical Methods for Heat & Fluid Flow*, 1(1), 31 – 49 (1991).

[17] T. S. Lee, Numerical experiments with fluid convection in tilted nonrectangular enclosures. *Numerical Heat Transfer*, 19(4), 487-499 (1991).

[18] M. Perić, Natural convection in trapezoidal cavities. *Numerical Heat Transfer, Part A: Applications*, 24(2), 213-219 (1993).

[19] H. Sadat, and P. Salagnac, Further results for laminar natural convection in a two-dimensional trapezoidal enclosure. *Numerical Heat Transfer, Part A: Applications*, 27(4), 451-459 (1995).

[20] R. A. Kuyper, and C. J. Hoogendoorn, Laminar natural convection flow in trapezoidal enclosures. *Numerical Heat Transfer, Part A: Applications*, 28(1), 55-67 (1995).

[21] M. Boussaid, A. Djerrada and M. Bouhadef, Thermosolutal transfer within trapezoidal cavity. *Numerical Heat Transfer: Part A: Applications*, 43(4), 431-448 (2003).

[22] F. Moukalled and M. Darwish, Natural convection in a trapezoidal enclosure heated from the side with a baffle mounted on its upper inclined surface. *Heat transfer engineering*, 25(8), 80-93 (2004).

[23] E. Natarajan, S. Roy and T. Basak, Effect of various thermal boundary conditions on natural convection in a trapezoidal cavity with linearly heated side wall (s). *Numerical Heat Transfer, Part B: Fundamentals*, 52(6), 551-568 (2007).

[24] M. Hammami, M. Mseddi and M. Baccar, Numerical study of coupled heat and mass transfer in a trapezoidal cavity. *Engineering Applications of Computational Fluid Mechanics*, 1(3), 216-226 (2007).

[25] E. Natarajan, T. Basak and S. Roy, Natural convection flows in a trapezoidal enclosure with uniform and non-uniform heating of bottom wall. *International Journal of Heat and Mass Transfer*, 51(3-4), 747-756 (2008).

[26] T. Basak, S. Roy and I. Pop, Heat flow analysis for natural convection within trapezoidal enclosures based on heat line concept. *International Journal of Heat and Mass Transfer*, 52(11-12), 2471-2483 (2009).

[27] N. I. Tracy and D. W. Crunkleton, Oscillatory natural convection in trapezoidal enclosures. *International Journal of Heat and Mass Transfer*, 55, 4498-4510 (2012).

[28] A. W. Mustafa and I. A. Ghani, Natural convection in trapezoidal enclosure heated partially from below. *Al-Khwarizmi Engineering Journal*, 8(1), 76-85 (2012).

[29] A. da Silva, É. Fontana, V. C. Mariani and F. Marcondes, Numerical investigation of several physical and geometric parameters in the natural convection into trapezoidal cavities, *International Journal of Heat and Mass Transfer*, 55, 6808-6818 (2012).

[30] M. M. Gholizadeh, R. Nikbakhti, J. Khodakhah and A. Ghasemi, Numerical study of double diffusive buoyancy forces induced natural convection in a trapezoidal enclosure partially heated from the right sidewall. *Alexandria Engineering Journal*, *55*(2), 779-795, (2016).

[31] K. Yazdani, M. Sahebjamei and A. Ahmadpour, Natural convection heat transfer and entropy generation in a porous trapezoidal enclosure saturated with power-law non-Newtonian fluids. *Heat Transfer Engineering*, *41*(11), 982-1001 (2020).

[32] K. G. B. M. Gowda, M. S. Rajagopal and K. N. Seethramu, Numerical studies on natural convection in a trapezoidal enclosure with discrete heating. *Heat Transfer Engineering*, 41(6-7), 595-606, (2019).

[33] S. C. Saha and M. M. K. Khan, A review of natural convection and heat transfer in attic-shaped space. *Energy Build*, 43, 2564-2571 (2011).

[34] S. W. Armfield and R. Street, The fractional-step method for the Navier-Stokes equations on staggered grids: the accuracy of three variations, *J. Comp. Phys*., 153, 660–665 (1999).

[35] S. W. Armfield and R. Street, An analysis and comparison of the time accuracy of fractional-step methods for the Navier Stokes equations on staggered grids, *Int. J. Numer. Methods Fluids*, 38, 255–282 (2002).

[36] S. Armfield and R. Street, A comparison of staggered and non-staggered grid Navier-Stokes solutions for the 8: 1 cavity natural convection flow. *ANZIAM Journal*, *46*, C918-C934 (2004).

[37] B. P. Leonard and S. Mokhtari, ULTRA-SHARP Non-oscillatory Convection Schemes for High-Speed Steady Multidimensional Flow, NASA TM 1-2568 (ICOMP-90-12). NASA Lewis Research Centre, 1990.

[38] P. G. Drazin and W. H. Reid, Hydrodynamic stability, Cambridge university press, 2004 Aug 5.

[39] J. B. McLaughlin and S. A. Orszag, Transition from periodic to chaotic thermal convection, *J. Fluid Mech*., 122, 123–142 (1982).

[40] S. Bhowmick, F. Xu, X. Zhang and S. C. Saha, Natural convection and heat transfer in a valley shaped cavity filled with initially stratified water, *Int. J. Therm. Sci*., 128, 59–69 (2018).

[41] H. Cui, F. Xu and S. C. Saha, A three-dimensional simulation of transient natural convection in a triangular cavity, *Int. J. Heat Mass Transf*., 85, 1012–1022 (2015).